NEURAL REGENERATION RESEARCH
March 2017, Volume 12, Issue 3
www.nrronline.org

RESEARCH ARTICLE

Guinea pigs as an animal model for sciatic nerve injury

Malik Abu Rafee[1], Amarpal[1,*], Prakash Kinjavdekar[1], Hari Prasad Aithal[1], Sajad Ahmad Wani[2], Irfan Ahmad Bhat[3]
1 Division of Surgery, Indian Veterinary Research Institute, Izatnagar, Bareilly, UP, India
2 Division of Veterinary Biotechnology, Indian Veterinary Research Institute, Izatnagar, Bareilly, UP, India
3 Division of Veterinary Physiology, Indian Veterinary Research Institute, Izatnagar, Bareilly, UP, India

How to cite this article: *Rafee MA, Amarpal, Kinjavdekar P, Aithal HP, Wani SA, Bhat IA (2017) Guinea pigs as an animal model for sciatic nerve injury. Neural Regen Res 12(3):452-457.*

Abstract
The overwhelming use of rat models in nerve regeneration studies is likely to induce skewness in treatment outcomes. To address the problem, this study was conducted in 8 adult guinea pigs of either sex to investigate the suitability of guinea pig as an alternative model for nerve regeneration studies. A crush injury was inflicted to the sciatic nerve of the left limb, which led to significant decrease in the pain perception and neurorecovery up to the 4th weak. Lengthening of foot print and shortening of toe spread were observed in the paw after nerve injury. A 3.49 ± 0.35 fold increase in expression of neuropilin 1 (*NRP1*) gene and 2.09 ± 0.51 fold increase in neuropilin 2 (*NRP2*) gene were recorded 1 week after nerve injury as compared to the normal nerve. Ratios of gastrocnemius muscle weight and volume of the experimental limb to control limb showed more than 50% decrease on the 30th day. Histopathologically, vacuolated appearance of the nerve was observed with presence of degenerated myelin debris in digestion chambers. Gastrocnemius muscle also showed degenerative changes. Scanning electron microscopy revealed loose and rough arrangement of connective tissue fibrils and presence of large spherical globules in crushed sciatic nerve. The findings suggest that guinea pigs could be used as an alternative animal model for nerve regeneration studies and might be preferred over rats due to their cooperative nature while recording different parameters.

Key Words: *nerve regeneration; Guinea pigs; animal model; sciatic nerve injury; foot print length; neuropilin; histopathology; neural regeneration*

***Correspondence to:**
Amarpal, MVSc, Ph.D., FNAVS, FISACP, FISVS,
amarpal@ivri.res.in.

orcid:
0000-0002-4827-3433 (Amarpal)

doi: *10.4103/1673-5374.202929*

Accepted: *2017-03-01*

Introduction
Sciatic nerve injury is the most frequently encountered peripheral nerve injury. Different animal models have been established to study the regenerative capacity of the peripheral nerve using various therapeutic agents (Ranjan et al., 2015). In rats, sciatic nerve crush injury model has been established to study various aspects of nerve regeneration (Algora et al., 1996; Daglioglu et al., 2010; Park et al., 2011; Raducan et al., 2013; Tamaddonfard et al., 2013; Tan et al., 2013). Induced sciatic nerve injury is manifested in limb weakness, altered gait and lengthening of foot prints (Khan et al., 2014). Foot prints are measured one day before and then at weekly interval after induction of the nerve injury for calculation of sciatic functional index (Santiago et al., 2009; Daglioglu et al., 2010; Raducan et al., 2013; Tamaddonfard et al., 2013). Extent of gastrocnemius muscle atrophy, measured as reduction in the ratio of muscle weight and/or volume of the gastrocnemius muscle of the experimental leg versus the control leg, has been used as an indirect indicator of the nerve injury (Santiago et al., 2009). Histopathological changes of sciatic nerve by light microscopy (Algora et al., 1996; Daglioglu et al., 2010; Park et al., 2011; Tamaddonfard et al., 2013; Tan et al., 2013; Bansode et al., 2014) and changes under scanning electron microscopic (SEM) examination (Tan et al., 2013) are the other important parameters studied to describe the changes following the injury and regeneration of sciatic nerve.

Rat and mice are the most common animal species used for models of nerve regeneration studies. Hilton et al. (2015) found a total of 284 *in vivo* studies on nerve regeneration, 222 were in rats and mice (78 %), 34 in rabbits (12 %), 11 in dogs, 6 in monkeys, 4 in sheep, 4 in cats and 3 in pigs. They considered that rats and mice are not the best models for the evolving complexities faced in designing nerve repair strategies. The preponderance of nerve regeneration data in a single species due to the overwhelming use of rat models in nerve regeneration is likely to skew treatment outcomes and leads to inappropriate evaluation of the risks and benefits.

Guinea pig is a popular laboratory animal and can be used as an alternative animal model in studies on sciatic nerve injury. Guinea pig being more docile in nature and easy to handle as compared to rats and mice can allow easy gait analysis and functional evaluation as well as recording of clinical parameters. In this study, we attempted to determine whether guinea pig can be an alternative to rat and mouse models for nerve degeneration/regeneration studies based on clinical parameters like pain perception and neurological recovery, histopathological and ultrastructural changes in nerve and associated muscle and changes in expression of certain genes.

Materials and Methods

Animals

Eight healthy guinea pigs (cavia porcellus) of either sex were used in this study. All the animals were provided with the standard diet, *ad libitum* water and allowed to acclimatize for approaching, handling and animal house conditions for a period of 10 days before initiation of the study. The study was approved by Institute Animal Ethics Committee of the Indian Veterinary Research Institute Vide order No.F.26-1/2015-16/J.D(R), dated 18th January, 2016.

Before induction of the injury, each animal was subjected to superficial and deep pain in order to assess the integrity of pain pathways and their response was graded using a 1–3 score scale (Tarlov and Klinger, 1954; **Table 1**). Similarly, neurological recovery score was recorded using ordinal scale of Tarlov and Klinger (1954) with slight modifications (**Table 1**). The total neurological recovery score was obtained by summing up pain perception and neurological recovery scores. The animals showing total neurological recovery score of 7 were assumed to have normal neurological function of the sciatic nerve and were included in the study.

Surgical intervention/procedure

The animals were anesthetized by intramuscular injections of xylazine (6 mg/kg) and ketamine (60 mg/kg) in the thigh muscles as per standard protocol. Left thigh region was prepared for aseptic surgery and the animal was secured in right lateral recumbency. A linear skin incision of 3–4 cm length was made at the caudo-lateral surface of the animal's left thigh and blunt dissection was performed to separate the biceps femoris and semitendinosus muscle to expose the sciatic nerve. Few drops of local anaesthetic (Lignocaine 2%) were instilled over the nerve to provide local analgesia. Five minutes later, the nerve was subjected to crush injury with the help of a curved hemostatic forceps (jaw width 3 mm). The strength used for compression was standardized at the second locking position of the hemostatic forceps (MICROSIDD INDIA) for 60 seconds. The site of the crush injury was the intermediate region of the sciatic nerve in its course down the thigh region before bifurcation into the tibial and peroneal nerves. The muscle and skin were sutured in standard manner. Postoperatively, all the animals were housed in individual boxes and administered with broad spectrum antibiotic enrofloxacin for 5 consecutive days and analgesic meloxicam for 3 days, intramuscularly. The skin wound was treated with povidone iodine until removal of skin sutures on the 10th postoperative day. Pain, neurorecovery and total neurological score were assessed in four animals on day 0 (before injury), day 1 (24 hours after injury) and then on the weekly interval up to 30 days.

Quantitative real-time PCR

To observe the response to injury at gene level, the expression level of well documented neuronal markers, neuropilin 1 (*NRP1*) and neuropilin 2 (*NRP2*), was estimated. Four animals were euthanized on the 7th day by intracardiac injection of over dosage of thiopental sodium. Injured (left limb) as well as normal (right limb) nerves were collected and immediately transferred to RNA later (Cat#R0901, Sigma, St. Louis, MO, USA) and stored at –80°C. Total RNA from the nerve sample was isolated using Trizol method (Invitrogen, Waltham, MA, USA). The purity and concentration of RNA was checked by a NanoDrop-2000 spectrophotometer (Thermo Fisher Scientific Inc., Wilmington, DE, USA). For synthesis of cDNA, 1 µg of RNA was reverse transcribed using a RevertAidTM First Strand cDNA Synthesis Kit (M/s MBI Fermentas Life Sciences, Maryland, USA) according to the manufacturer's protocol. Real time-PCR was performed using SYBR Green-I master mix (SYBR Green chemistry), a two-step RT-PCR kit (Brilliant III Ultra-Fast SYBR® Green QPCR Master Mix #600882) with 7500 fast instrument (Applied Biosystem). Each PCR reaction mix (10 µL) consisted of 5 µL of SYBR Green PCR Master mix, 2.0 (10 ng) µL of cDNA, 0.1 µL each of forward and reverse primers (10 pmol/µL, **Table 2**) , 0.15 µL passive reference dye (1:500) and 2.45 µL of NFW. Each reaction was carried out in triplicate with non-template control (NTC) for each gene. Amplification and detection of specific products were performed with the following cycle profile: one cycle of 95°C for 3 minutes, and 40 cycles of 94°C for 3 seconds, 60°C for 30 seconds, with one final cycle of standard dissociation curve. The passive reference dye ROX™ was used for normalization of the reporter signal (SYBR Green). Beta-actin was employed as the internal/endogenous control. A melting curve analysis was performed to know the specificity of qPCR. For the test genes and endogenous control, tenfold serial dilution was run in the study to estimate the efficiency of PCR, and the percentage efficiency ranged between 90% and 110%. Four samples in each group and each sample in triplicates were run (4 biological replicates × 3 technical replicates) per PCR run. The results were analyzed by $^{\Delta\Delta}$Ct or delta delta cycle threshold (Livak and Schmittgen, 2001) method as per the formula: $\Delta\Delta Ct = [(Ct_{target} - Ct_{internal\ control})\ sample - (Ct_{target} - Ct_{internal\ control})\ calibrator)]$. The change in the gene expression was calculated as $2^{-\Delta\Delta Ct}$ (Livak and Schmittgen 2001).

Print length (PL) and toe spread (TS)

On the 30th day, foot PL and TS were recorded in four animals. The foot PL was measured as the distance from the tip of the third toe to the most posterior aspect of the paw. The TS was measured as the distance from the 1st to the 3rd toe.

Weight and volume of gastrocnemius muscle

The animals were then euthanized and crushed nerve and the gastrocnemius muscle of the both limbs were collected. Ratios of the gastrocnemius muscle weight and volume of experimental limb to control limb were calculated from three animals.

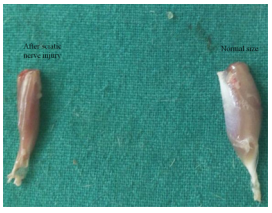

The gastrocnemius muscle of experimental limb (left) is thinner than that of control limb (right).

Figure 1 Gross difference in size of the gastrocnemius muscle of experimental (left) and control limbs (right) of guinea pigs.

Table 1 Pain and neurorecovery scores

Score	
Pain perception scores	
1	No reaction to forceful compression (absence of deep pain)
2	Mild reaction to forceful compression of the toe (absence of superficial pain but presence of deep pain)
3	Strong reaction to light compression (superficial pain intact)
Neurorecovery scores	
1	Complete paralysis: complete loss of sensation below the stifle joint except medial aspect
2	Lifted animal shows extension of the hock joint, absence of web paw. While walking/sitting, there is lateral deviation/abduction of the limb, knuckling of the paw
3	Lifted animal shows angulations (flexion) of the hock joint, web paw. While walking/sitting, there is slight lateral deviation/abduction, slight knuckling of the paw
4	Normal positioning of the limb while walking/sitting

Table 2 Primers used for quantitative real-time PCR

Gene	Primer	Sequence (5'–3')	Accession number	Amplicon size (bp)
NRP-1	Forward	GAA TCT ACC CTG AGC GAG CC	XM_005003202.2	102
	Reverse	CAT TGG GAG TTG TCG GTC CA		
NRP-2	Forward	GGA GGT CGC CTG AAT TCC AA	XM_005005763.2	167
	Reverse	AAC CTT AAG TCC GCT GGA GG		
Beta-actin	Forward	ACT CCT CCA CAG AGG AAG GC	NM_001172909.1	170
	Reverse	AGT TGG GGG ACA AAA AGG GG		

Table 3 Scores of pain perception, neurorecovery, and total neurological recovery

	Day 0	Day 1	Day 7	Day 14	Day 21	Day 28
Pain	3.00±0.00	1.00±0.38*	1.00±0.54*	2.00±0.54*	2.00±0.00*	2.00±0.00*
Neurorecovery	4.00±0.00	1.00±0.38*	1.00±0.38*	1.00±0.38*	2.00±0.49*	2.00±0.49*
Total neurological recovery	7.00±0.00	2.00±0.49*	3.00±0.76*	3.00±0.76*	4.00±0.49*	4.00±0.49*

Data are expressed as the mean ± SD. *$P < 0.05$, *vs.* day 0.

Table 4 *NRP1* and *NRP2* gene expression, print length, toe spread, and ratios of gastrocnemius muscle weight and volume of experimental (injured) limb to control (normal) limb

	Normal side	Injured side
Sciatic nerve		
NRP1 gene expression	–0.99±0.33	–2.79±1.02*
NRP2 gene expression	–2.34±0.30	–3.40±1.60
Limb		
Print length (cm)	3.195±0.115	3.653±0.306*
Toe spread (cm)	1.718±0.164	0.921±0.187**
Ratio of gastrocnemius muscle weight of experimental limb to control limb	0.369±0.027	
Ratio of gastrocnemius muscle volume of experimental limb to control limb	0.384±0.105	

Data are expressed as the mean ± SD ($n = 4$). *$P < 0.05$, **$P = 0.01$, *vs.* normal side. NRP: Neuropilin.

Histopathology of nerve and muscle samples

The samples collected were stored in 10 % formalin to evaluate the microstructural changes. The nerve sample from the fourth animal was stored in 2.5% glutaraldehyde to observe ultrastructual changes using scanning electron microscopy. Two of the formalin fixed muscle and nerve samples were processed by paraffin embedding and cut into 4–5 μm thick sections and stained with hematoxylin and eosin. The third formalin fixed nerve sample was processed for Marchi's technique (Marchi, 1886) for assessment of myelin degeneration in one sample. For this purpose, the formalin fixed specimen was post-chromed for 5 days in 3% potassium dichromate and then transferred to Marchi's fluid for 15 days. Thereafter, the specimen was processed by paraffin embedding and cut into 4–5 μm thick slices. One slide was subjected to hematoxylin-eosin staining and the other observed as such for histopathological changes.

Scanning electron microscopy

The nerve sample preserved in 2.5% glutaraldehyde was post

fixed in 2% OsO_4, washed with distilled water and then dehydrated through a graded series of ethanol from 30%, 50%, 70%, 90% to 100%. The dehydrated specimen was critical point dried and mounted on aluminium stub in longitudinal orientation, using adhesive silicon tape, sputter coated with Au-Pd (80:20) and then visualized using FEI Quanta 250 scanning electron microscope (Houston, TX, USA).

Statistical analysis

All data were statistically analyzed using SPSS 16.0 software (SPSS, Chicago, IL, USA) with one-way analysis of variance and are expressed as the mean ± SD. $P < 0.05$ was considered statistically significant.

Results

Clinical observations

Before the injury, pain pathways were fully intact for both superficial and deep pain. 24 hours after the injury, the score of pain decreased significantly from the normal and it remained significantly decreased until the 4th weak, though there was some improvement in the score from the 2nd week onwards (**Table 3**). The similar pattern was observed in neurological recovery and total neurological recovery score. The animals were cooperative while recording the parameters.

Quantitative real-time PCR (changes in gene expression)

Cycle threshold (Ct) values of target genes were normalized to internal reference β-actin. Normalized gene expression data from biological replicates were averaged and calibrated against the normal nerve; $\Delta\Delta Ct = [(Ct_{target} - Ct_{internal\ control})$ sample – $(Ct_{target} - Ct_{internal\ control})$ calibrator)]. Expression of *NRP1* was significantly increased in the tested nerve ($\Delta\Delta Ct = -2.79 \pm 1.02$) as compared to its expression in the normal nerve ($\Delta\Delta Ct = -0.99 \pm 0.33$). The expression of *NRP2* gene was appreciable but statistically non-significantly higher in the tested nerve ($\Delta\Delta Ct = -3.40 \pm 1.6$) as compared to its expression in the normal nerve ($\Delta\Delta Ct = -2.34 \pm 0.30$) (**Table 4**). There was 3.49 ± 0.35 fold increase in NRP1 gene and 2.09 ± 0.51 fold increase in *NRP2* gene 1 week after the nerve injury as compared to the normal nerve.

Changes in weight and volume of gastrocnemius muscle

Grossly the mass of the normal gastrocnemius muscle appeared greater than the muscle of the test limb on the 30th day (**Figure 1**). Ratios of gastrocnemius muscle weight and volume of experimental limb to control limb 30 days after sciatic nerve injury are shown in **Table 4**.

PL and TS

Lengthening of foot print and shortening of toe spread were observed in guinea pigs after injury to the sciatic nerve. Data of PL of the paw in right (normal) and left (experimental) limbs are shown in **Table 4**. The difference was significant ($P < 0.05$). TS in the right (normal) and left (experimental) limb are shown in **Table 4**. The difference was highly significant ($P = 0.01$).

Histopathological changes in nerve and muscle

Vacuolated appearance of the nerve was observed. Different types of vacuoles ranging from vacuolated foci-containing eosinophilic material and associated with a distorted cell nucleus to larger, multilocular, linear array of compartmentalized myelin debris (digestion chambers) (**Figure 2B**) were observed. Degenerated myelin stained black after Marchi's staining, whereas normal myelin stained light brown. The degenerated myelin was found as aggregates/deposits (**Figure 2C**). Combining Marchi's staining and hematoxylin and eosin staining procedures revealed the presence of degenerated myelin deposits in digestion chambers (**Figure 2D**). Hematoxylin and eosin stained sections of gastrocnemius muscle samples showed absence of striations, multinucleated myofiber and degenerative changes (**Figure 3B**). In longitudinal sections, the muscle fibers were shirked, broken and wiggly. Areas of myofibril fragmentation and rupture (called retraction caps) were observed. Eosinophillic homogenous, hypercoagulated myofibers (hyalinization) indicating degeneration was also observed. Spaces between the muscle bundles were widened. In crosssections, angular (triangular) and shirked bundles were observed. Hyalinization of the muscle bundles was also evident.

Ultra-structural changes in the nerve

Scanning electron microscopy revealed loose and rough arrangement of connective tissue fibrils and presence of large spherical globules in the degenerating fibers oriented along the major axis of the nerve on day 30 (**Figure 4**).

Discussion

In an earlier study, Park et al. (2011) showed that the expression of neuronal markers was increased 1 week after nerve injury. The same was observed in this study with regard to the expression of *NRP1* and *NRP2* genes. *NRP2* and *NRP1* are members of a well-documented class of receptors that respond to ligands, termed semaphorins, of which there are a number of subclasses (Rore and Piischel, 2003). NRP1 and *NRP2* each responds to selective members of subclass-3 semaphorins, secreted proteins that guide migration of axonal growth cones to their appropriate target tissue during development (Kitsukawa et al., 1997; Kolodkin et al., 1997; Bagnard et al., 2000). A marked induction, at the messenger ribonucleic acid (mRNA) level, of *NRP2* in Schwann cells within the crush site and distal stumps of crushed rodent nerves has been reported earlier (Scariato et al., 2003; Ara et al., 2004).

Locomotion is a well co-ordinated event that requires precise timing (speed) of impulse conduction to get meaningful movements. Demyelination by means of crush injury may alter this normal coordination as action potential could be delayed and movements become uncoordinated (Zachary, 2007). Impaired coordinated movements and decreased pain perception and decreased recovery scores noticed in the present study might be attributed to demyelination and delayed action potential caused by crush injury.

The ratios of gastrocnemius muscle weight and volume of experimental limb to control limb indicate more than 50 % weight and volume loss 30 days after nerve injury. Previous

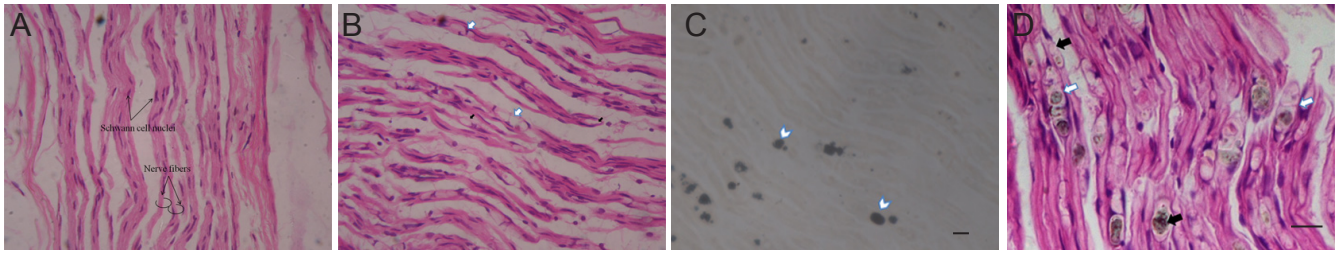

Figure 2 Histopathological changes observed in guinea pigs 30 days after sciatic nerve injury.
(A) Photomicrograph of normal nerve in longitudinal section (hematoxylin-eosin staining) depicting Schwann cell nuclei and nerve fibers. (B) Photomicrograph of crushed nerve in longitudinal section (hematoxylin-eosin staining). Black arrows indicate vacuolated, larger, multilocular foci containing less intense eosinophilic material and associated with a distorted cell nucleus and white arrows indicate digestion chambers as larger, multilocular, linear array compartmentalized myelin diebrisin which myelin debris can be seen. (C) A section stained with Marchi's stain showing degenerated myelin as black deposits (indicated by white arrow heads) and normal (un-degenerated) myelin stained light brown (Marchi's staining). (D) Marchi's staining and hematoxylin-eosin staining reveals vacuoles (black arrows) and digestion chambers (white arrows) filled with dark stained degenerated myelin. Scale bars: 100 μm.

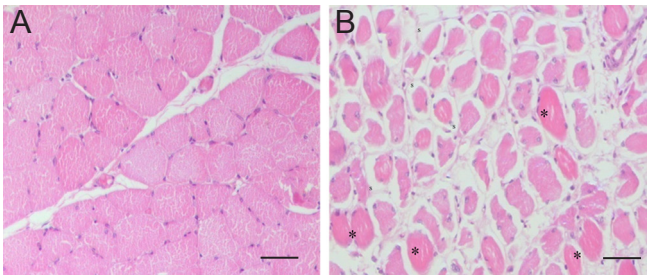

Figure 3 Histopathological changes in gastrocnemius muscle in guinea pigs 30 days after sciatic nerve injury.
(A) Photomicrograph of normal gastrocnemius muscle (hematoxylin-eosin staining). (B) Photomicrograph of degenerative changes in gastrocnemius muscle (hematoxylin-eosin staining). Asterisks (*) indicate eosinophillic-homogenous-hypercoagulated myofibers (hyalinization), and S indicates shrinkage and clear fat filled spaces at the periphery of muscle fibers and angular fibers can be seen. Scale bars: 100 μm.

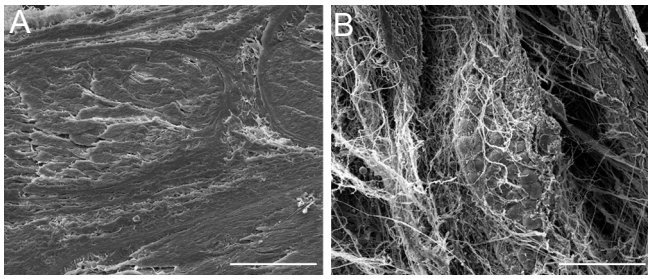

Figure 4 Ultrastructural changes in sciatic nerve in guinea pigs 30 days after sciatic nerve injury.
(A) Scanning electron micrograph of normal sciatic nerve. (B) Scanning electron micrograph of crushed site of the sciatic nerve of guinea pigs on the 30th day on the longitudinal section. Compared with normal sciatic nerve, there is loose and rough arrangement of connective tissue fibrils and spherical globules in the crushed sciatic nerve. Scale bars: 200 μm.

studies also reported significant reduction in the muscle weight in rats after nerve injury (Higashino et al., 2013). Khan et al. (2014) reported lengthening of foot prints in rats after nerve injury. Bain et al. (1989) reported increased PL and decreased TS in rats after complete sciatic nerve lesion. Similar findings were noticed in guinea pigs after sciatic nerve injury in the present study. Previous studies have observed that TS represents the major alteration after sciatic nerve injury and may be used alone as an indicative of the sciatic nerve injury stage (Walker et al., 1994; Bervar, 2000; Baptista et al., 2007).

Histology is a traditional method to evaluate degeneration/regeneration of the nerves. The response of the peripheral nervous system following injury varies with the cause and extent of the injury, and different pathological changes depend on the degree of injury. After sciatic nerve injury, Wallerian degeneration occurs in the distal stump consisting of a series of processes, including axonal degeneration, myelin degeneration and disintegration, Schwann cell proliferation, infiltration of macrophages and mast cells, and axonal and myelin debris clearance (Dubovy, 2011). In the present study, histological examination of regenerated nerves was done by conventional hematoxylin-eosin staining, Marchi's staining and combined Marchi's and hematoxylin-eosin staining protocols. Hematoxylin-eosin staining of nerve revealed the presence of vacuoles, gitter (foamy) cells and digestion chambers indicating phagocytosis and lysosomal degradation of myelin by Schwann cells and/or haematogenous macrophages. These different types of vacuoles gave the tissue a vacuolated appearance. The degenerated myelin was found as black aggregates/deposits after Marchi's staining. These black aggregates were found in digestion chambers and vacuoles on pre-treated samples with Marchi's procedure followed by hematoxylin-eosin staining procedure. Similar changes have been observed in rat nerve injury models (Holtzman and Novikoff, 1965; Amniattalab et al., 2010; Khan et al., 2014; Gomez-Sanchez et al., 2015). The gastrocnemius muscle is supplied by the sciatic nerve and crush injury would lead to quick atrophy of the muscle. Atrophic changes in gastrocnemius muscle could be correlated with the degeneration in sciatic nerve. Similar histopathogical changes have been observed in rats after nerve injury (Higashino et al., 2013).

Electron microscopy enables analysis of the ultra-structural events associated with Wallerian degeneration and peripheral nerve regeneration (Ohmi, 1961). The normal myelinated axons are seen as relatively smooth cylindrical structures which interweave with strands of collagen and elastic fibers that course over their length. The axons vary in diameter and are closely packed within the nerve bundles. After degen-

eration, the myelin sheaths of nerve fibers are distorted and swollen with numerous cytoplasmic bulges occurring along the length of the degenerating axons. The amount of the connective tissue covering the damaged fibers was increased due to which the axons have lost their smooth appearance. Many degenerating fibers began to fragment into large spherical globules which were oriented in a linear fashion along the major axis of the nerve. Similar changes have been observed in rat nerve injury model (Gershenbaum and Roisen, 1978).

The functional, macroscopic, microscopic and ultrastructural changes observed in sciatic nerve and gastrocnemius muscle changes in guinea pigs mimic the alterations observed in rat and other species following sciatic nerve injury. Further, the assessment of functional parameters like pain perception, neurological recovery and TS and PL was facilitated by cooperative nature and the larger size of the guinea pigs as compared to rats and mice. Taken together, guinea pigs can prove to be an alternative model for sciatic nerve regeneration studies, which can address to the problem of overwhelming use of rat models in nerve regeneration and thereby reduce the skew in treatment outcomes.

Acknowledgments: *Authors are highly thankful to Indian Council of Agriculture Research and the Director of Indian Veterinary Research Institute for providing necessary facilities.*
Author contributions: *MAR, A, PK and HPA conceived and carried out the work. SAW and IAB carried out real-time PCR. All authors read and approved the final version of this paper.*
Conflicts of interest: *None declared.*
Plagiarism check: *This paper was screened twice using CrossCheck to verify originality before publication.*
Peer review: *This paper was double-blinded and stringently reviewed by international expert reviewers.*

References

Algora J, Chen, LE, Seaber AV, Wong GH, Urbaniak JR (1996). Functional effects of lymphotoxin on crushed peripheral nerve. Microsurgery 17:131-135.
Ara J, Bannerman P, Hahn A, Ramirez S, Pleasure D (2004). Modulation of sciatic nerve expression of class 3 semaphorins by nerve injury. Neurochem Res 29:1153-1159.
Bagnard D, Thomasset N, Lohrum M, Püschei AW, Boiz J (2000). Spatial distributions of guidance molecuies regulate chemorepulsion and chemoattraction of growth cones. J Neurosci 20:1030-1035.
Bain JR, Mackinnon SE, Hunter DA (1989) Functional evaluation of complete sciatic, peroneal and posterior tibial nerve lesions in the rat. Plast Reconstr Surg 83:129-138.
Bansode VJ, Vyawahare NS, Munjal NB, Gore PN, Amrutkar PS, Sontakke SR (2014) Ameliorative effect of ethyl pyruvate in neuropathic pain induced by chronic constriction injury of sciatic nerve. Indian J Pain 28:82-88.
Baptista AF, Gomes JR, Oliveira JT, Santos SM, Vannier-Santos MA, Martinez AM (2007) A new approach to assess function after sciatic nerve lesion in the mouse - adaptation of the sciatic static index. J Neurosci Methods 161:259-264.
Bervar M (2000) Video analysis of standing—an alternative footprint analysis to assess functional loss following injury to the rat sciatic nerve. J Neurosci Meth 102:109-116.
Daglioglu E, Berker M, Demirci M, Tuncel M, Karabulut E, Tuncel A (2010) Microscopic and electrophysiological changes on regenerating sciatic nerves of rats treated with simvastatin. Folia Neuropathol 48:49-56.
Dubovy P (2011) Wallerian degeneration and peripheral nerve conditions for both axonal regeneration and neuropathic pain induction. Ann Anat 193:267-275.
Gershenbaum MR, Roien FJ (1978) A scanning electron microscopic study of peripheral nerve degeneration and regeneration. Neuroscience 3:1241-1250.
Gomez-Sanchez JA, Carty L, Iruarrizaga-Lejarreta M, Palomo-Irigoyen M, Varela-Rey M, Griffith M, Hantke J, Macias-Camara N, Azkargorta M, Aurrekoetxea I, De Juan VG, Jefferies HB, Aspichueta P, Elortza F, Aransay AM, Martínez-Chantar ML, Baas F, Mato JM, Mirsky R, Woodhoo A, Jessen KR (2015) Schwann cell autophagy, myelinophagy, initiates myelin clearance from injured nerves. J Cell Biol 210:153-168.
Higashino K, Matsuura T, Suganuma K, Yukata K, Nishisho T, Yasui N (2013) Early changes in muscle atrophy and muscle fiber type conversion after spinal cord transection and peripheral nerve transection in rats. J Neuroeng Rehabil 10:46.
Hilton MK, Prakhar M, Joachim K (2015) The overwhelming use of rat models in nerve regeneration research may compromise designs of nerve guidance conduits for humans J Mater Sci 26:226.
Holtzman E, Novikoff AB (1965) Lysozomes in the rat sciatic nerve following crush. J Cell Biol 27:651-669.
Khan AA, Faruqi NA, Ansari MS (2014) Effects of hydrocortisone on the sciatic nerve crush injury in adult rat-a light microscopic study. Curr Neurobiol 5:11-16.
Kitsukawa T, Shimizu M, Sanbo M, Hirata T, Taniguchi M, Bekku Y, Yagi T, Fujisawa H (1997) Neuropilin-semaphorin III/D-mediated chemorepulsive signals play a crucial role in peripheral nerve projection in mice. Neuron 19:995-1005
Kolodkin AL, Levengood DV, Rowe EG, Tai YT, Giger RJ, Ginty DD (1997) Neuropilin is a semaphorin III receptor. Cell 90:753-762.
Livak KJ, Schmittgen TD (2001). Analysis of relative gene expression data using real time quantitative PCR and the 2-ΔΔCt. Methods 25:402-408.
Marchi V (1886) Sulle degenerazioni consecutive all' estirpazione totale e parziale del cervelletto. Riv Sper Freniat 12:50-56.
Ohmi S (1961) Electron microscopic study on Wallerian degeneration of the peripheral nerve. Z Zellforsch 54:39-67.
Park SS, Byeon YE, Ryu HH, Kang BJ, Kim Y, Kim WH, Kang KS, Han HJ, Kweon OK (2011) Comparison of canine umbilical cord blood-derived mesenchymal stem cell transplantation times: involvement of astrogliosis, inflammation, intracellular actin cytoskeleton pathways, and neurotrophin-3. Cell Transplant 20:1867-1880.
Răducan A, Mirică S, Duicu O, Răducan S, Muntean D, Fira-Mlădinescu O, Lighezan R (2013) Morphological and functional aspects of sciatic nerve regeneration after crush injury. Rom J Morphol Embryol 54:735.
Ranjan P, Mazumder PM, Parmaguru R, Sasmal D, Sinha RK, Aggarwal Y, Das J (2015) Effect of ethyl acetate fraction of the aerial parts of salvia splendens. Sellow ex Roem. and Schult on Diabetic Neuropathy. Pharmacologia 6:313-323.
Rore R, Piischel AW (2003) The function of semaphorins during nervous system development. Front Biosci 8:84-99.
Santiago LY, Clavijo-Alvarez J, Brayfield C, Rubin JP, Marra KG (2009) Delivery of adipose-derived precursor cells for peripheral nerve repair. Cell Transpl 18:145-158.
Scariato M, Ara J, Bannerman P, Scherer S, Pieasure D (2003) Induction of neuropilins-1 and -2 and their ligands, Sema3A, Sema3F, and VEGF, during Wallerian degeneration in the peripheral nervous system. Exp Neurol 183:489-498.
Tamaddonfard E, Farshid AA, Ahmadian E, Hamidhoseyni A (2013) Crocin enhanced functional recovery after sciatic nerve crush injury in rats Iran J Basic Med Sci 16:83-90.
Tan CW, Ng MH, Ohnmar H, Lokanathan Y, Nur-Hidayah H, Roohi SA, Naicker AS (2013) Sciatic nerve repair with tissue engineered nerve: Olfactory ensheathing cells seeded poly (lactic-co-glygolic acid) conduit in an animal model. Indian J Orthop 47:547-552.
Tarlov IM, Klinger H (1954) Spinal cord compression studies: II. Time limits for recovery after acute compression in dogs. AMA Arch Neurol Psychiatry 71:271-290.
Walker JL, Evans JM, Meade P, Resig P, Sisken BF (1994) Gait-stance duration as a measure of injury and recovery in the rat sciatic nerve model. J Neurosci Methods 52:47-52.
Zachary JF (2007) Nervous system. In: Pathologic basis of veterinary disease. 4th Edition (McGavin MD, Zachary JF, eds). Mosby Elsevier, St. Louis, Missouri.

Copyedited by Li CH, Song LP, Zhao M